CMS MET Performance in Events Containing Electroweak Bosons from pp Collisions at $\sqrt{s} = 7$ TeV

Stefano Lacaprara[1] and Artur Apresyan[2]

[1]INFN Padova, [2]CALTECH

JetMet meeting
CERN, 25 June 2010

Title and abstract

CMS MET Performance in Events Containing Electroweak Bosons from pp Collisions at $\sqrt{s} = 7$ TeV
JME-10-005

During the spring of 2010, the LHC delivered proton-proton collisions with a centre-of-mass energy of 7 TeV. In this note, we present results of studies of missing transverse energy, as measured by the CMS detector, in events containing W bosons, Z bosons or isolated, high transverse momentum photons. The performance of several different MET reconstruction algorithms is compared.

Editors: Artur Apresyan, Stefano Lacaprara; Senior editor: Jim Alexander

Details

Seven supporting AN

- **AN-2010/118** CMS MET Performance in Events Containing Electroweak Bosons decaying into muons from pp Collisions at $\sqrt{s} = 7$ TeV
- **AN-2010/131** Type-I and Type-II CaloMET performances in 7TeV data
- **AN-2010/132** MET Scale Validation with Photon + Jet Events (TTU)
- **AN-2010/133** MET significance performance on early CMS collision data (Cornell)
- **AN-2010/176** Commissioning of the missing transverse energy in $W \to \mu\nu$ events for 12 nb^{-1} with the pp center-of-mass energy of $\sqrt{s} = 7$ TeV
- **AN-2010/197** Studies on Missing Transverse Energy for events with muons
- **AN-2010/202** Missing transverse energy performances with electroweak bosons decaying into electrons in pp collisions at $\sqrt{s} = 7$ TeV

Timescale

Approval

- PAS and AN freezing: **Saturday, June 26** TOMORROW
- *light* Pre-approval: **Monday, June 28**
- Approval: **Friday, July 09**

ARC

Fabio Cossutti (Trieste)
Sharon Lee Hagopian (Florida-state)
(chair) Paraskevas Sphicas (CERN)

Overview

Sections

- Introduction
- The CMS Detector
- Description of Missing Transverse Energy algorithms
- Data Sample Definition and Selection
- $\not\!\!E_T$ in Photon + Jet Events
- $\not\!\!E_T$ reconstruction in events with a W
- Performance of $\not\!\!E_T$ reconstruction in events with a Z boson
- Comparison of Z and γ results
- Effects of muon reconstruction uncertainties on $\not\!\!E_T$
- $\not\!\!E_T$ significance
- Estimating the $\not\!\!E_T$ distribution in $W \rightarrow e\nu$ events

Introduction

- The CMS Detector
  - usual stuff

    The central feature of the Compact Muon Solenoid (CMS) apparatus is a superconducting solenoid . . .
- Description of Missing Transverse Energy algorithms
  - Some details and references on Calo$\not\!\!E_T$, type-I, type-II correction, Tc$\not\!\!E_T$ and Pf$\not\!\!E_T$.
- Data Sample Definition and Selection
  - General event selection (good lumi, scraping, cleaning, . . .)
  - Description of MC simulation

$\not{E}_T$ in Photon + Jet Events

- ECAL energy deposit $\Delta R < 0.4 < 4.2 + 0.004 \times q_T$.
- HCAL energy deposit $\Delta R < 0.4 < 2.2 + 0.001 \times q_T$.
- Ratio HCAL/ECAL $\Delta R < 0.15 < 0.05$.
- N. tracks $\Delta R < 0.4 < 3$.
- $R9 > 0.9 \times E^\gamma$
- γ cluster major and minor 2^{nd} moments in $0.20 - 0.35$, $0.15 - 0.3$.
- $\eta_{width} < 0.03$
- $q_T > 10$ and $|\eta| < 1.479$ (Barrel)

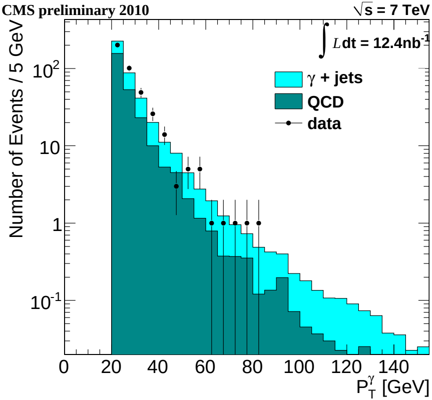

Figure: P_T spectrum for isolated photon events from data and the predicted contributions from Monte Carlo simulation of direct photon production and from dijet production events containing a jet misidentified as a photon.

Significant QCD background, but jet are mostly *e.m.* (π^0), so scale fine anyhow

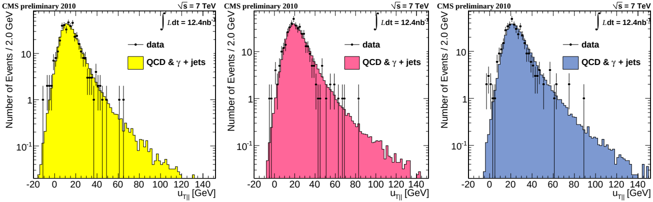

Figure: Component of recoil parallel to the direction of the photon p_T in photon plus jet event: for CaloMet, pfMet and tcMet: Data vs MC simulation.

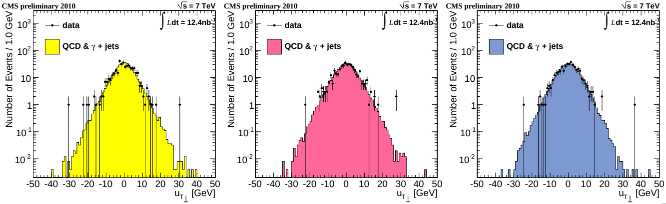

Figure: Component of recoil perpendicular to the direction of photon p_T in photon plus jet events: for CaloMet, pfMet and tcMet: Data vs MC

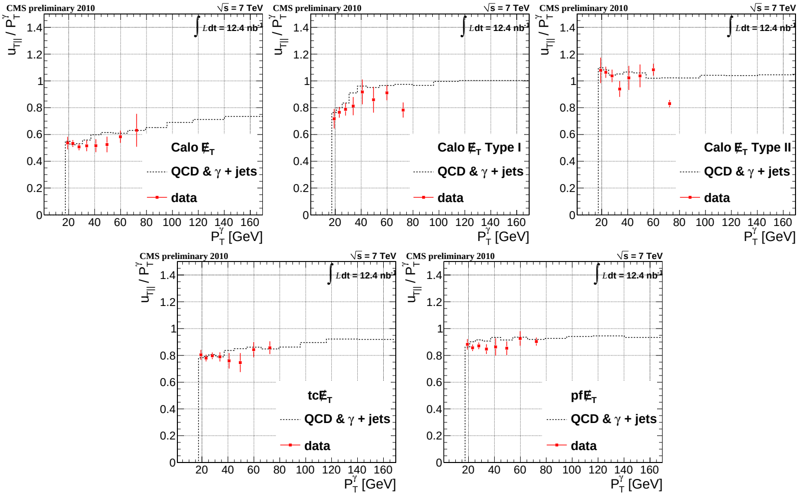

Figure: Ratio between the component of recoil parallel to the direction of the photon p_T to the photon p_T versus the magnitude of photon p_T in photon plus jet events: for Calo$\not\!\!E_T$, type-I Calo$\not\!\!E_T$ and type-II Calo$\not\!\!E_T$, tc$\not\!\!E_T$ and pf$\not\!\!E_T$: Data vs MC simulation.

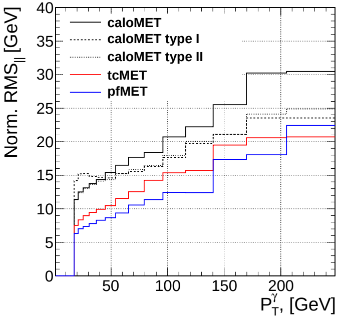

Figure: Resolution on the component of the recoil parallel (left) and perpendicular (right) to the photon after correcting for scale

$\not\!\!E_T$ reconstruction in events with a W

$W \to \mu\nu$

- HLT $p_{\mathrm{T}}(\mu) > 9$ GeV
- Good quality muon $p_{\mathrm{T}} > 25$ GeV (and $p_{\mathrm{T}} > 15$ GeV for a QCD enriched sample)
- $|\eta_\mu| < 2.1$.
- Combined relative isolation $\Sigma(p_T^{tracks} + E_T^{ecal} + E_T^{hcal})/p_{\mathrm{T}}^{\mu} < 0.15$
- No second muon $p_{\mathrm{T}} > 10$ GeV

$W \to e\nu$

- HLT $p_{\mathrm{T}}(e) > 10$ GeV
- Electron id 80% efficiency.
- GSF filter + supercluster $p_{\mathrm{T}} > 25$ GeV (no looser cut due to larger qcd backgound)
- $|\eta_e| < 2.5$ excluding $1.4442 < |\eta| < 1.56$
- η dependent isolation on ECAL, HCAL and tracks
- No second electron $p_{\mathrm{T}} > 20$ GeV

$M_{\mathrm{T}} > 50$ GeV applied for final selection

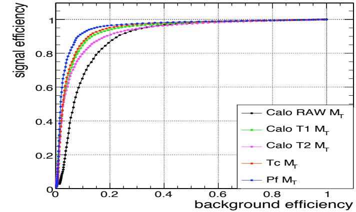

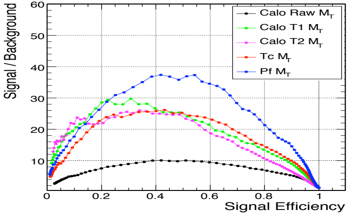

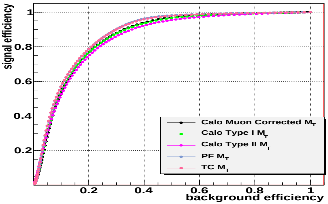

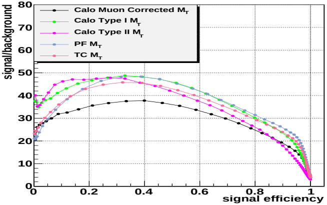

ϵ_S vs ϵ_B for $W \to e\nu$ (up) and $W \to \mu\nu$ (bottom)

(S vs B) for $W \to e\nu$ (up) and $W \to \mu\nu$ (bottom)

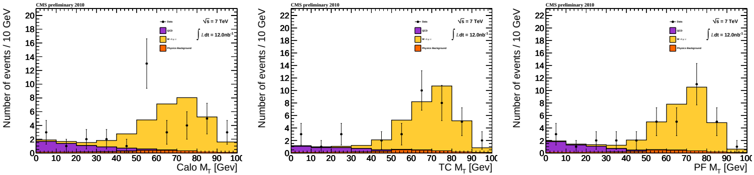

(a) Type-II Calo$\not\!\!E_T$ (b) Tc$\not\!\!E_T$ (c) Pf$\not\!\!E_T$

Figure: M_{T} distribution in $W \to \mu\nu$ with tight muon p_T cut

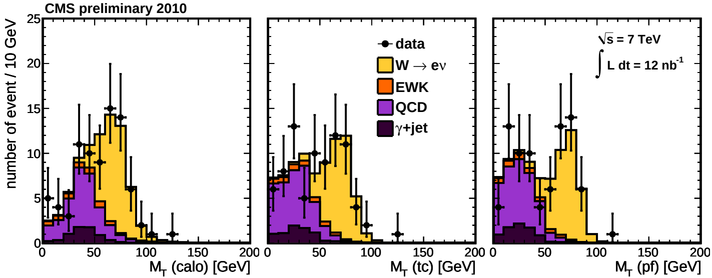

Figure: M_{T} distribution in $W \to e\nu$ candidate events

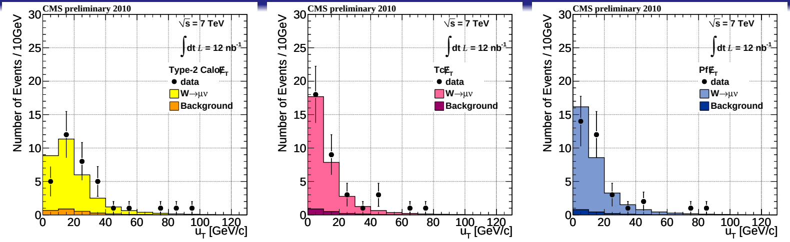

(a) Type-II Calo$\not\!\!E_T$ (b) Tc$\not\!\!E_T$ (c) Pf$\not\!\!E_T$

Figure: recoil distribution in $W \to \mu\nu$

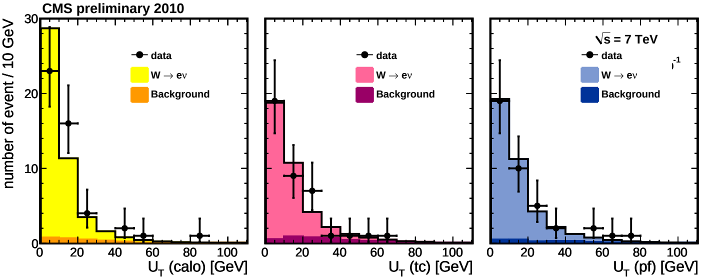

Figure: recoil distribution in $W \to e\nu$

Performance of $\not\!\!E_T$ reconstruction in events with a Z boson

$Z \rightarrow \mu\mu$

- HLT $p_{\mathrm{T}}(\mu) > 9$ GeV
- Two Good quality muons $p_{\mathrm{T}} > 20$ GeV
- $|\eta_\mu| < 2.1$.
- Tracker absolute $\Sigma(p^{tracks}) < 3$ GeV
- $M_{\mu\mu} > 60$ GeV applied for final selection.

$Z \rightarrow ee$

- HLT $p_{\mathrm{T}}(e) > 10$ GeV
- Electron id 95% efficiency.
- Two good electron (GSF filter + supercluster) $p_{\mathrm{T}} > 20$ GeV
- $|\eta_e| < 2.5$ excluding $1.4442 < |\eta| < 1.56$
- η dependent isolation on ECAL, HCAL and tracks
- shower shape selection
- $M_{ee} > 40$ GeV applied for final selection.

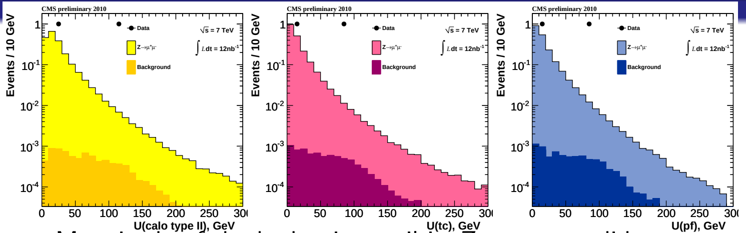

Figure: Magnitude of the hadronic recoil in $Z \to \mu\mu$ candidate events for CaloMet, pfMet and tcMet: Data vs MC simulation.

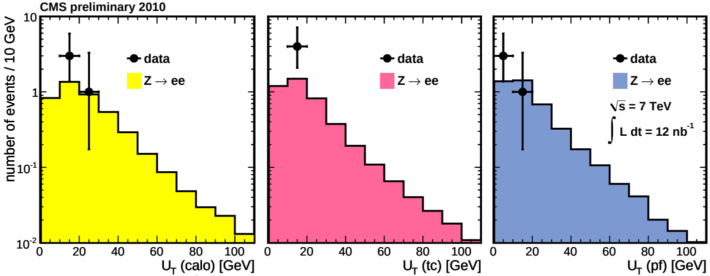

Figure: Magnitude of the hadronic recoil in $Z \to ee$ candidate events for CaloMet (left), tcMet (center) and pfMet (right) : Data vs MC simulation.

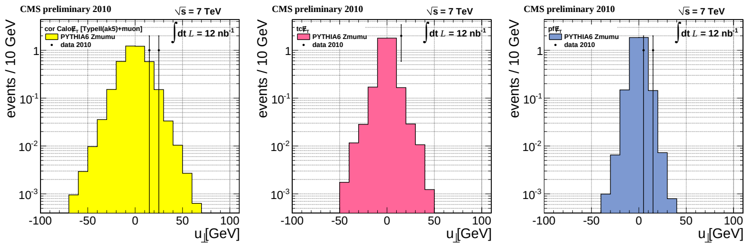

Figure: Component of recoil perpendicular to the direction of q_T in $Z \rightarrow \mu\mu$ candidate events: for CaloMet, pfMet and tcMet vs MC simulation

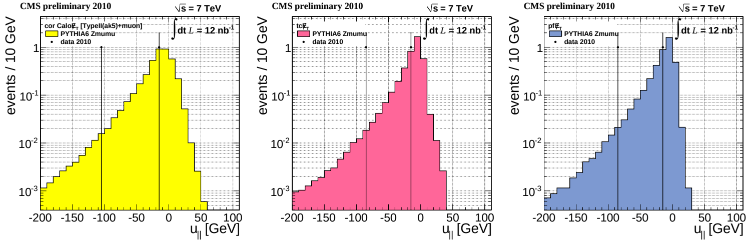

Figure: Component of recoil parallel to the direction of Q_T in $Z \rightarrow \mu\mu$ candidate events: for CaloMet, pfMet and tcMet vs MC simulation

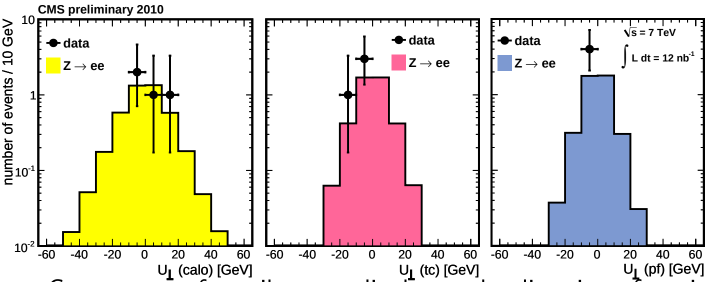

Figure: Component of recoil perpendicular to the direction of q_T in $Z \rightarrow ee$ candidate events: for Calo$\not\!\!E_T$, tc$\not\!\!E_T$ and pf$\not\!\!E_T$

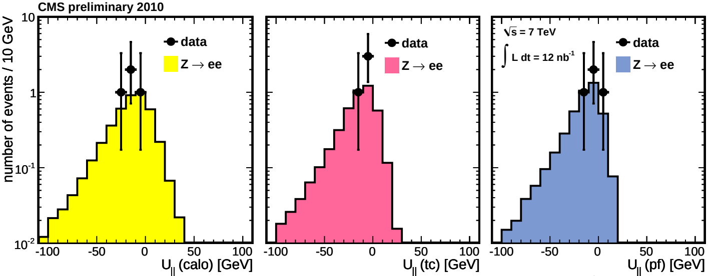

Figure: Component of recoil parallel to the direction of Q_T in $Z \rightarrow ee$ candidate events: for CaloMet (left), tcMet (center) and pfMet (right) vs

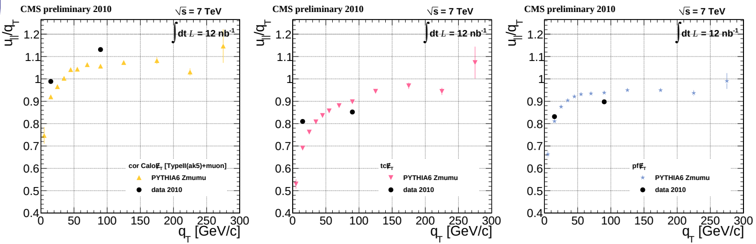

Figure: Ratio between $u_{||}/Q_{||}$ versus Q_T in $Z \to \mu\mu$ candidate events: for CaloMet, pfMet and tcMet vs MC simulation

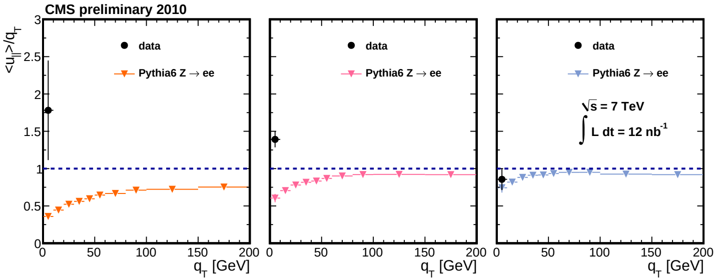

Figure: Ratio between $u_{||}/Q_{||}$ versus Q_T in $Z \to ee$ candidate events: for CaloMet (left), tcMet (center) and pfMet (right) vs MC simulation

Comparison of Z and γ results

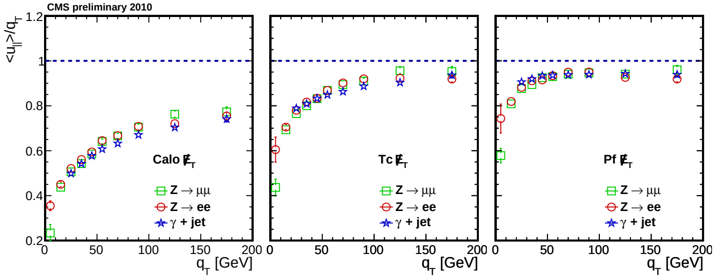

Figure: Comparison of response in photon and Z events for raw CaloMET (left), tcMET (center) and pfMET (right).

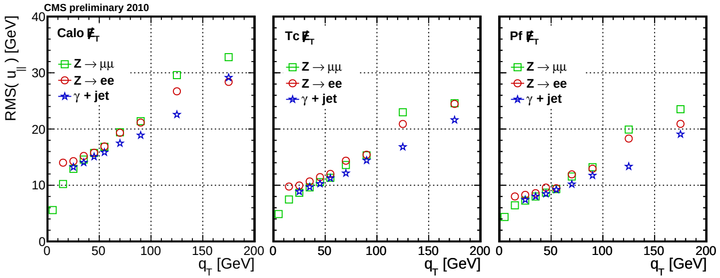

Figure: Comparison of parallel resolution of recoil in photon and Z events for raw CaloMET (left), tcMET (center) and pfMET (right).

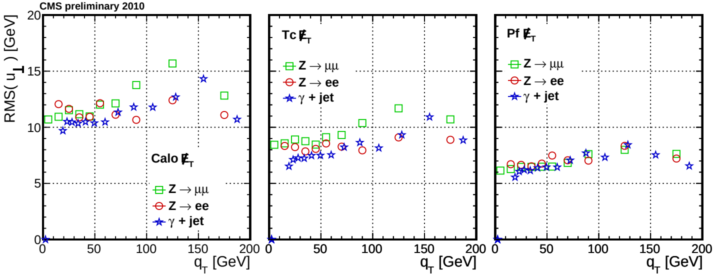

Figure: Comparison of perpendicular resolution of recoil in photon and Z events for raw CaloMET (left), tcMET (center) and pfMET (right).

$\not{E}_T$ significance

Build likelihood function for $\not{E}_T$ compomenent (gaussian error)

$$\mathcal{L}_i(\vec{\varepsilon}_i) \sim \exp\left(-\frac{1}{2}\vec{E}_{T\,i}{}^{T}\mathbf{V}_i^{-1}\vec{E}_{T\,i}\right)$$

$\mathbf{V}_i$ covariance matrix
Significance as the log-likelihood ratio:

$$\mathcal{S} \equiv 2\ln\left(\frac{\mathcal{L}(\vec{\varepsilon} = \vec{\not{E}}_T^{\text{observed}})}{\mathcal{L}(\vec{\varepsilon} = 0)}\right),$$

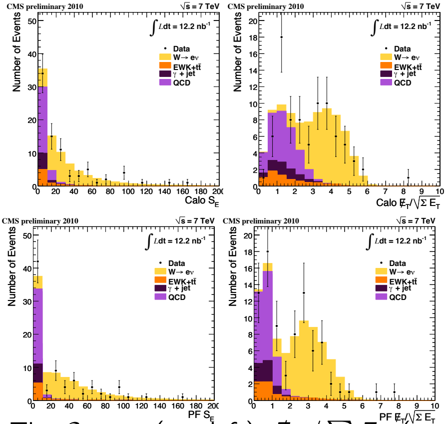

Figure: The $\mathcal{S}_{calo\not{E}_T}$ (top left), $\not{E}_T/\sum E_T$ (top right), $\mathcal{S}_{PF\not{E}_T}$ (bottom left) and $PF\not{E}_T/PF\sum E_T$ (bottom right) distributions in $W \to e\nu$ events. All samples have been normalized to 10 pb^{-1}.

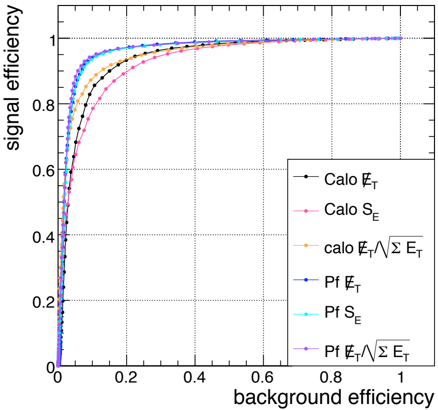

Figure: Signal efficiency versus background efficiency for six possible discriminant variables.

Effects of muon reconstruction uncertainties on $\not{E}_T$

Simulate with present MC a muon distortion and see the effect on $\not{E}_T$ and M_{T} for $W \to \mu\nu$ candidates.

Example with $1 \cdot 10^{-3}$ [1/ GeV] ($3 \cdot 10^{-3}$ [GeV]) for $1/p_{\mathrm{T}}$ (p_{T}), respectively.

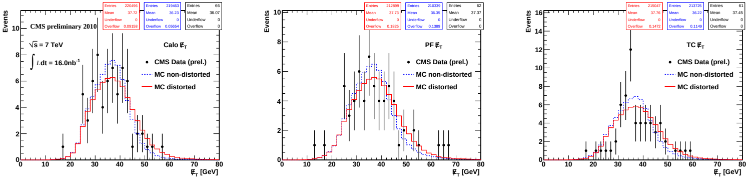

Figure: Missing Transverse Energy distribution for W events using CaloMet (top left), tcMet (top right) and pfMet (bottom). The data are shown as full dots. The red histograms correspond to the MC distributions with distortions applied to the muon momentum, in order to mimic residual tracking misalignments, inaccurate magnetic field or inactive material in the simulation. The dashed blue line displays the MC distribution using the default reconstruction of the muon momentum.

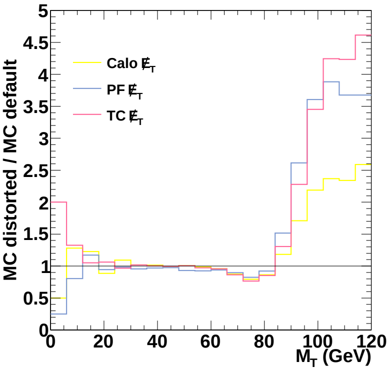

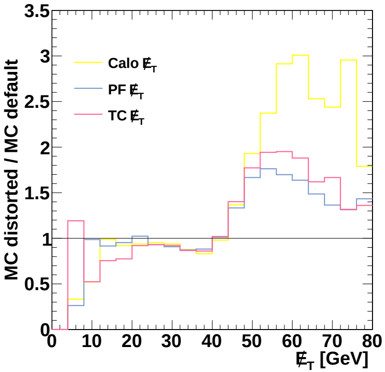

Figure: The effect of the distortions on the W transverse mass (left) and $\not\!\!E_T$ (right) using the three types of $\not\!\!E_T$: ratio of distorted to non-distorted MC distributions. Results are shown for CaloMet, pfMet and tcMet.

Estimating the $\not\!\!E_T$ distribution in $W \to e\nu$ events

- $u_{\|}$ and $u_{\perp}$ recoil modeled as Gaussian distributions, means widths functions of p_T^W.
- convolve p_T^W (from MC) with the parametrized recoil functions to generate PDFs for the inclusive $u_{\|}$ and $u_{\perp}$ distributions :

$$f(u_i; p^W) = (Kp^W_{T\,,i} + C) \otimes \sigma(1 + Bp^W_{T\,,i})$$

- Fit parameters of recoil model with pure W sample (large $\not\!\!E_T$ ot M_{T})
- Chech parameters by comparing the predicted $\not\!\!E_T$
- Use parameters uncertainties to estimate syst on W shape

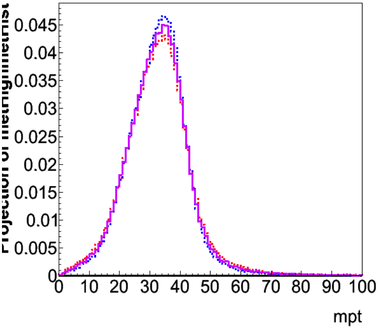

Figure: Expected W $\not\!\!E_T$ Shape Uncertainties for $0.1\ \mathrm{pb}^{-1}$

Z *ersatz* aka Z *morphing*. Proof of principle and hard reality.

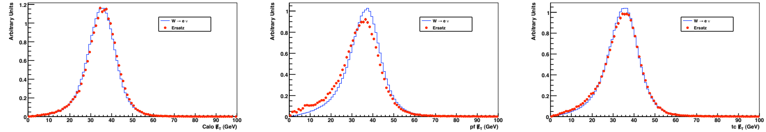

Figure: Comparison of the emulated $W \to e\nu$ $\not\!\!E_T$ distribution with the reconstructed $W \to e\nu$ $\not\!\!E_T$ distribution in MC for CaloMet, pfMet and tcMet as a proof of principle for the estimation.

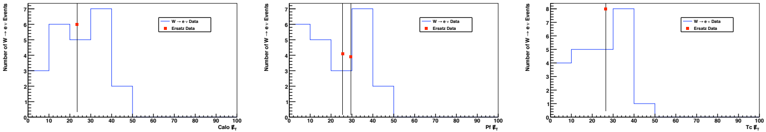

Figure: Comparison of the emulated $W \to e\nu$ $\not\!\!E_T$ distribution with the reconstructed $\not\!\!E_T$ distribution of $W \to e\nu$ selected events in 9.03nb^{-1} of data for CaloMet, pfMet and tcMet .

Conclusion

- Only γ+jet has (limited) statistics, few tens of W and handful of Z.
- Hard to draw any conclusion.
- A lot of work from all groups involved in this PAS
  Thanks!
- Need to keep up-to-date with incoming statistcs (when available ...)
- Must be ready to populate all plots with more events as they arrive.
- Lot of work ahead of us, still